Steady-state and time-resolved investigations of a crown thioether conjugated with methylacridinium and its complexes with metal ions

Tiziana del Giacco, Benedetta Carlotti, Stefano De Solis, Arianna Barbafina and Fausto Elisei*

Received 3rd August 2010, Accepted 1st November 2010
DOI: 10.1039/c0cp01411g

The crown thioether 9-[4-(4,7,10,13-tetrathia-1-azacyclopentadecyl]phenyl-*N*-methylacridinium perchlorate (TCMA) was synthesized and characterized with the aim to verify its ability to interact selectively with metal ions and substantiate the possibility to detect easily the presence of heavy metals in fluid samples. The spectroscopic properties of TCMA, alone and in the presence of metal ions, were therefore studied in polar solvents (MeCN and H_2O); in particular, steady-state UV-Vis spectrophotometric and fluorimetric techniques were used together with transient absorption spectroscopy with fs time resolution to investigate the spectral and dynamic properties of the lowest excited singlet state of TCMA and of TCMA/metal ion complexes. The absorption in the Vis region is characterized by a charge-transfer nature with the methylacridinium moiety acting as the electron-acceptor and the anilic group as the electron-donor. No emission from the S_1 was detected both in MeCN and H_2O, while a small $S_2 \rightarrow S_0$ fluorescence emission (λ_{max} = 485 nm and ϕ_F = 0.0011) was detected in water. Time-resolved measurements with fs resolution of TCMA in MeCN have shown that the relaxed S_1 state is reached ~0.6 ps after the laser pulse, while the $S_1 \rightarrow S_0$ time constant is 3.7 ps. Among the investigated metal ions, only Fe^{3+} (in MeCN) and Hg^{2+} (in MeCN and H_2O) were able to form stable complexes (association constant, K_{ass} = 1–11 × 10^4 M^{-1}) with TCMA. The S_1 state of the TCMA/M^{n+} complexes emits with low quantum yield (ϕ_F = 0.0023–0.014) and decays with time constants much longer than TCMA itself, at least in the case of TCMA/Hg^{2+} in MeCN. This study showed that TCMA is a good candidate for colorimetric/fluorimetric sensing of Hg^{2+} in aqueous media owing to its high selectivity towards metal ions.

Introduction

Chemosensors are compounds that modify significantly their electrical, electronic, magnetic and/or optical properties by interaction with specific guests. Due to the development of fluorescent and chromogenic chemosensors able to reveal quickly, selectively and sensitively polluting species, much attention has been paid in the use of spectroscopic techniques to reveal the presence of metal ions in samples of various nature.[1–4] In fact, most fluorescent sensors mainly based on photoinduced electron transfer (PET) and internal charge transfer (ICT) processes are used for *in vitro* and *in vivo* cellular imaging to make this approach more promising than other analytical methods. Thus, a number of fluorescent sensors have been successfully used to reveal the presence of calcium,[5–7] copper,[8–11] mercury[12–20] and zinc[21,22] in solution and in cells. This interest is due to the bioactivity of these heavy metals and/or their ability to induce diseases even in a short period of time. In particular, disorders of calcium metabolism occur when the body has too little or too much calcium;[23] copper can cause gastrointestinal disturbance (short-term) and liver or kidney damage (long-term);[24] bioaccumulation of mercury has been linked with minamata, myocardial infarction and some kinds of autism and can lead to damages of the brain, kidneys, central nervous system, immune system, and endocrine system;[25,26] zinc is one of the most abundant transition metals in the brain whose excess release may occur in a variety of pathological conditions which may contribute to a selective neuronal cell death.[27]

In spite of the wide scientific activity regarding the detection of metal ions in various media, a detailed investigation of the detection mechanism and of the photophysical and dynamic properties of sensor/metal ion complexes is actually missing.

This work deals with the synthesis and characterization of a crown thio-ether (9-[4-(4,7,10,13-tetrathia-1-azacyclopentadecyl]-phenyl-*N*-methylacridinium perchlorate, TCMA) by steady-state absorption and emission techniques and transient absorption spectroscopy with femtosecond time-resolution (Scheme 1). The ability of TCMA to interact with metal ions, particularly stable and selective for Fe^{3+} and Hg^{2+}, was investigated by recording the spectral and kinetic properties in the presence of numerous cations in MeCN and H_2O.

Experimental section

Starting materials

All the reagents were obtained from commercial suppliers (Aldrich, Fluka) and used as received. Hg^{2+}, Fe^{3+}, Na^{+},

Chemistry Department, and Centro di Eccellenza sui Materiali Innovativi Nanostrutturati (CEMIN), University of Perugia, via Elce di Sotto 8, 06123 Perugia, Italy. E-mail: elisei@unipg.it; Fax: +39 075-5855598; Tel: +39 075-5855588

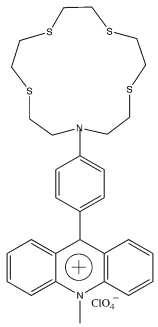

Scheme 1 9-[4-(4,7,10,13-tetrathia-1-azacyclopentadecyl]phenyl-*N*-methylacridinium perchlorate (TCMA).

Li^+ and Mg^{2+} were used as perchlorate salts, Ca^{2+}, Ba^{2+},Co^{2+}, Ni^{2+}, Pb^{2+} and Cu^{2+} as nitrate salts, Cs^{2+} as chloride and Fe^{2+} as ammonium sulfate. Dimethylformamide (DMF, Aldrich) and tetrahydrofuran (THF, Aldrich) were purified and dried by standard procedures.[28] Acetonitrile (MeCN, Fluka, for UV spectroscopy) was used as received.

Instrumental analysis

^{1}H-NMR spectra were run on a Bruker AC 200 (200 MHz) spectrometer from solutions in $CDCl_3$ with TMS as internal standard. GC-MS analyses were performed on a Hewlett Packard 6890A gas-chromatograph (HP-Innovax capillary column, 15 m) coupled with a MSD-HP 5973 mass selective detector (70 eV). GC analyses were carried out on a HP 5890 gas-chromatograph using a HP-Innovax capillary column, 15 m. HPLC analyses were performed with a liquid chromatograph HP 1100.

Synthesis of 9-[4-(4,7,10,13-tetrathia-1-azacyclopentadecyl] phenyl-*N*-methylacridinium perchlorate (TCMA)

TCMA was synthesized in five steps, starting from aniline commercially available. Firstly, *N*,*N*-di(2-hydroxyethyl)aniline was prepared by reaction of aniline with 2-chloroethanol in water.[29] The diol was converted by *para*-toluenesulfonyl chloride in the corresponding tosylate in $NaOH/H_2O/THF$, *N*,*N*-bis[2-(*para*-toluenesulfonyl)ethyl]aniline:[30] ^{1}H-NMR ($CDCl_3$, 200 MHz): δ 7.73 (d, 4H), 7.26 (d, 4H), 7.15 (t, 2H), 6.70 (t, 1H), 6.44 (d, 2H), 4.18 (t, 4H), 3.46 (t, 4H), 2.42 (s, 3H). This product was added, together with 3,6-dithiaoctane-1,8-dithiol (prepared as previously described)[31] in a mixture of $CsCO_3$ in DMF to produce the receptor, 1-phenyl-4,7,10,13-tetrathia-1-azacyclopentadecane.[30] ^{1}H-NMR ($CDCl_3$, 200 MHz): δ 7.28 (dd, 2H), 6.73 (m, 3H), 3.57 (t, 4H), 2.73 (m, 16H). The reaction of the receptor with *N*-methylacridinium iodide (prepared as previously described)[32] in the presence of I_2 in DMF, after elaborate workup of the crude, produced TCMA.[33] ^{1}H-NMR ($CDCl_3$, 200 MHz) δ 8.52 (d, 2H), 8.28 (d + t, 4H), 7.89 (t, 2H), 7.45 (d, 2H), 7.07 (d, 2H), 4.75 (s, 3H), 3.72 (t, 4H), 2.84 (m, 16H).

Photophysical measurements

Absorption spectra were recorded with a Perkin-Elmer Lambda 800 spectrophotometer. Fluorescence emission spectra were measured with a Fluorolog-2 (Spex, F112AI) spectrophotofluorimeter. Fluorescence quantum yields (experimental error of *ca.* 7%) were determined from the emission spectra of the samples recorded at an absorbance smaller than 0.1 at the excitation wavelength, to avoid self-absorption effects, by use of anthracene in ethanol as reference (ϕ_F = 0.22).[34]

The transient behavior on the ultrafast time scale was investigated by use of femtosecond pulses generated by an amplified titanium-sapphire laser system (Spectra Physics, Mountain View, CA)[35–37] that produces 1 W pulses centred at 800 nm at a repetition rate of 1 kHz. Pump pulses centred at 400 nm were obtained by second harmonic generation in a 500 μm β-barium-borate crystal. In the transient absorption set-up (Helios, Ultrafast Systems) the pump pulses were passed through a chopper which cut out every second pulse and collimated to the sample in a 2 mm quartz cuvette. Probe pulses for optical measurements were produced by passing a small portion of 800 nm light through an optical delay line (with a time window of 1600 ps) and focusing into a 2 mm thick Ti:Sapphire window to generate a white-light continuum in the 430–800 nm window. The white light was focused onto the sample and the chirp inside the sample cell was determined by measuring the laser-induced Kerr signal of the solvent. The temporal resolution of our time-resolved spectroscopic technique is ~150 fs while the spectral resolution is 1.5 nm. All the measurements were carried out under magic angle in order to avoid the rotational decay processes, in a 2 mm cell and at an absorbance of about 0.5 at 400 nm. The solution was stirred during the experiments to avoid photodegradation processes. Transient Absorption Data were analyzed using the Surface Xplorer PRO (Ultrafast Systems) software. It was possible to visualize the 3D and 2D data surfaces, to simultaneously display and save multiple spectra and kinetics, to perform temporal chirp corrections, to make time zero adjustments, to fit the kinetics by exponential(s) and perform instrumental response function deconvolution, to perform Singular Value Decomposition (SVD)[38,39] of the 3D surface into principal components (spectra and kinetics) and to perform Global Analysis.

Transient kinetics on the time scale of several microseconds were collected by a nanosecond laser flash photolysis setup previously described (Nd:YAG Continuum, Surelite II, third harmonics, λ_{exc} = 355 nm, pulse width *ca.* 7 ns and energy $\leq$1 mJ per pulse).[40,41] All measurements were carried out at room temperature; the solutions were saturated by bubbling with nitrogen.

Ground-state absorption spectra were recorded before and after the transient absorption measurements to check for photodegradation.

Quantum mechanical calculations

Quantum mechanical calculations were performed using the CAChe 7.5 software. Transition energies and oscillator strengths were obtained by INDO/1-CI calculations[42] after geometrical optimization with the PM3 semiempirical model.[43,44] Electron excitations (singly excited) from the 20 highest occupied to the 20 lowest virtual molecular orbitals (MO) were used.

Results and discussion

Absorption and emission properties of TCMA

Absorption. The $S_0 \rightarrow Sn$ absorption spectra of TCMA in H_2O and MeCN are shown in Fig. 1. The bands recorded in H_2O are centred at about 350, 410 and 528 nm with relatively high absorption coefficients (in the range of 3700–17 000 M^{-1} cm^{-1}, Table 1). In MeCN, the hypsochromic bands were characterized by the same absorption maxima and slightly smaller molar absorption coefficients (~2700 and 15 000 M^{-1} cm^{-1}, Table 1). Instead, the broad band in the Vis region shows significant bathochromic and hyperchromic effects on going to the aprotic solvent MeCN (Fig. 1). This is in agreement with the charge-transfer nature of the first absorption band which is due to the presence of a strong electron-donor substituent (such as the anilic group *N*,*N* substituted with the crown thio-ether) linked to the 9 position of the methylacridinium moiety. Taking into account the electron-acceptor properties of the excited acridinium moiety (E°_{red} = 2.32 V)[45] and the electron-donor properties of *N*,*N* alkyl-substituted anilic group (E°_{ox} < 1 V),[46] it is reasonable that the lowest excited singlet state of TCMA has a charge-transfer nature. As a matter of fact, the charge-transfer band associated with the *N*,*N*-diethylaniline/*N*-methylacridinium complex is reported to be centred at 570 nm.[47] Furthermore, the hypsochromic effect recorded in H_2O for the Vis band can be ascribed to the stronger interaction between the solvent and the anilic nitrogen of TCMA which reduces the electron transfer efficiency from the anilic group to the methylacridinium moiety and then destabilizes the lowest excited singlet state.

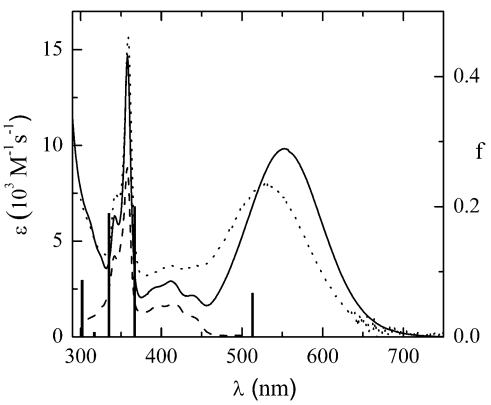

Fig. 1 Absorption spectra of TCMA in MeCN (solid line) and H_2O (dotted line) and of MA in MeCN (dashed line) together with the oscillator strengths (*f*) obtained by INDO/1-CI calculations (vertical bars).

It has to be noted that the spectral behaviour of TCMA is close to that already reported for a similar compound where the crown thio-ether is replaced by a crown ether.[48]

The experimental data can be compared with the absorption maxima and oscillator strengths obtained by quantum-mechanical calculations using the INDO/1-CI method (see Tables 1 and 2). Taking into account that no solvent effects were included in the calculations, the predicted transition energies are in good agreement with the experimental results. Each absorption band is due to an allowed $\pi \rightarrow \pi^*$ transition (oscillator strength f = 0.067–0.20). The first transition is mainly described by the HOMO $\rightarrow$ LUMO configuration with charge transfer character, where HOMO and LUMO are located in correspondence of the anilic (AN) and methylacridinium (MA) moieties, respectively. Instead, the other two transitions are characteristic of the methylacridinium moiety ($\pi_{MA} \rightarrow \pi^*_{MA}$), as also shown by a comparison of the absorption spectra of MA and TCMA shown in Fig. 1.

Emission. The lowest excited singlet state of TCMA with CT character does not show fluorescence in MeCN and H_2O. In fact, a fluorescence quantum yield ϕ_F smaller than 10^{-4} was estimated upon excitation at 550 nm. Furthermore, a fluorescence signal characterized by an emission spectrum centered at 485 nm (ϕ_F = 0.0011 at λ_{exc} = 358 nm) and an excitation spectrum close to that of MA (Fig. 2) were detected in H_2O. The spectral characteristics of this emission suggest that it is originated from the S_2 state of methylacridinium character; thus, in this solvent the radiative $S_2 \rightarrow S_0$ process is able to compete with the $S_2 \rightarrow S_1$ internal conversion, also in

Table 2 Absorption maxima (λ_{max}) and oscillator strengths (*f*) of the lowest $S_0 \rightarrow S_n$ transitions of TCMA calculated by INDO/1-CI

Compound	Transition	λ_{max}/nm	Nature	*f*
TCMA	$S_0 \rightarrow S_1$	513	$\pi_{AN} \rightarrow \pi^*_{MA}$	0.067
	$S_0 \rightarrow S_2$	367	$\pi_{MA} \rightarrow \pi^*_{MA}$	0.20
	$S_0 \rightarrow S_3$	335	$\pi_{MA} \rightarrow \pi^*_{MA}$	0.19
	$S_0 \rightarrow S_4$	317	$\pi_{AN} \rightarrow \pi^*_{MA}$	0.007
	$S_0 \rightarrow S_5$	302	$\pi_{AN} \rightarrow \pi^*_{AN}$	0.087

Table 1 Spectral properties of TCMA in the absence and in the presence of additive, together with the C_{50} parameter, the association equilibrium constants and the fluorescence quantum yields

Solvent	Additive	λ^{abs}_{max}/nm	ε/M^{-1} cm^{-1}	C_{50} (10^{-5} M)	K_{ass} (10^4 M^{-1})	λ^{em}_{max}/nm	ϕ_F
MeCN	—	358	14 460	—	—	—	<0.0001
	—	412	2890	—	—	—	—
	—	552	9830	—	—	—	—
	Fe^{3+}	361	—	2.5	1.0	510	0.014
	—	423	—	—	—	—	—
	Hg^{2+}	362	—	3.0	4.2	506	0.0023
	—	426	—	—	—	—	—
H_2O	—	359	16 650	—	—	485	0.0011
	—	412	3730	—	—	—	—
	—	528	7790	—	—	—	—
	Hg^{2+}	361	—	0.75	11	506	0.0040
	—	427	—	—	—	—	—

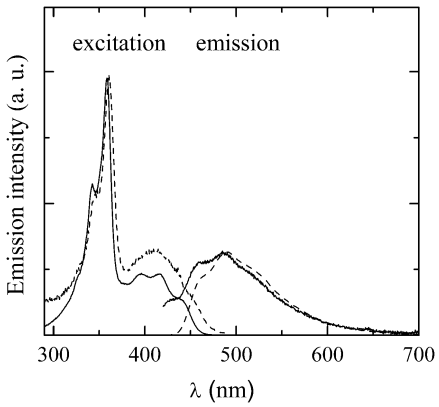

Fig. 2 Fluorescence excitation (λ_{em} = 480 nm) and emission spectra (λ_{exc} = 358 nm) of TCMA (solid lines) and MA (dashed lines) in H_2O.

agreement with the higher absorption coefficient recorded at 412 nm in H_2O (Table 1). The lifetimes of the singlet excited states of TCMA are very short and were characterized by fs time-resolution absorption spectroscopy (see below).

Spectral properties in the presence of metal ions

The ability of TCMA to interact with metal ions was investigated by recording steady-state absorption and emission spectra in unbuffered water solutions and in MeCN, in the presence of increasing amounts of salts of alkali metals (Li^+, Na^+, and Cs^+), alkaline earth metals (Mg^{2+}, Ca^{2+}, and Ba^{2+}), transition metals (Co^{2+}, Ni^{2+}, Fe^{2+}, Fe^{3+}, Cu^{2+}, Zn^{2+} and Hg^{2+}) and poor metals (Pb^{2+}). The experiments have shown that TCMA is able to interact selectively with Hg^{2+} (in both the solvents) and Fe^{3+} (only in MeCN); in fact, the other metal ions were not able to modify the absorption and emission spectra of TCMA even at rather high concentrations (up to $\sim 3 \times 10^{-4}$ M). This selective behaviour of TCMA can be compared with those of analogous crown ethers.[48] In fact, the replacement of oxygen atoms (*hard* type) with sulfur atoms (*soft* type) in the crown structure decreases the electrostatic interactions between the thio-ether and the metal ions, and then the affinity for metals, owing to the smaller charge density in the S atoms.[49]

Absorption. Upon addition of the perchlorate salts of Fe^{3+} (in MeCN) and Hg^{2+} (in MeCN and H_2O) the absorption spectra of TCMA show important changes in shape which form isosbestic points in the 460–470 nm region (Fig. 3). The absorption spectra were particularly affected above 450 nm where the $S_0 \rightarrow S_1$ band practically disappears at high ion concentrations. On the contrary, the intensities of the absorption bands due to the $S_0 \rightarrow S_2$ and $S_0 \rightarrow S_3$ increase with the ion concentration while their position is practically unchanged. These findings indicate that there is a TCMA-ion interaction (likely 1 : 1) which affects mainly the lowest excited singlet state with charge-transfer character.

Linear trends of the ratio A_0/A (where A_0 and A represent the absorbance in the absence and in the presence of the cation, respectively) were recorded at 550 nm in MeCN and 530 nm in H_2O in the presence of increasing amounts of Fe^{3+} and Hg^{2+}.

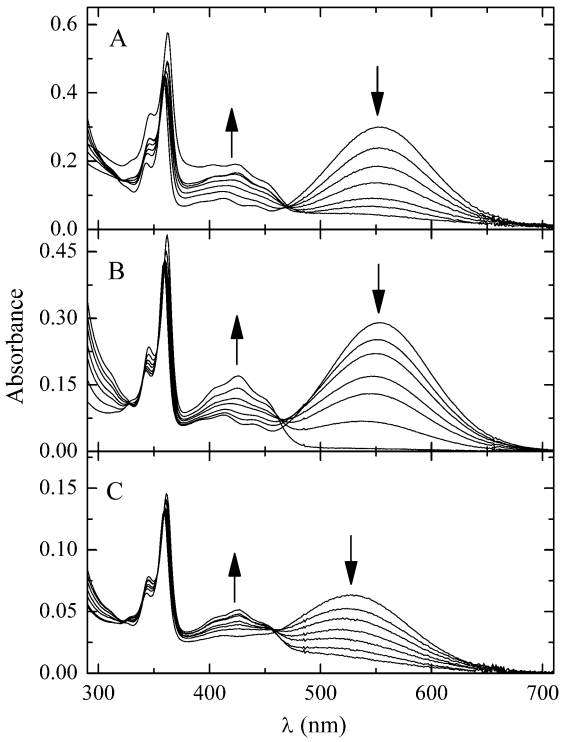

Fig. 3 Absorption spectra of TCMA in MeCN (3.0×10^{-5} M) in the presence of (A) $Fe(ClO_4)_3$ (0–8.8×10^{-5} M) and (B) $Hg(ClO_4)_2$ (0–5.7×10^{-5} M) and (C) in H_2O (8.0×10^{-6} M) in the presence of $Hg(ClO_4)_2$ (0–2.7×10^{-5} M).

Table 1 shows the metal ion concentration (C_{50}) able to halve the absorbance of free TCMA.

Emission

The addition of Fe^{3+} and Hg^{2+} to TCMA also induced a fluorescence enhancement: in general the spectral shape remains always unstructured in the presence of salts but there was an important variation in the fluorescence intensity (Fig. 4). The effects of the metal ions are slightly different and merit a comment. In fact, the fluorescence spectrum of the TCMA–Fe^{3+} complex in MeCN is centred at 510 nm and its shape does not change with the ion concentration (Fig. 4A). Instead, the emission spectrum of the TCMA–Hg^{2+} complex in MeCN is centred at $\sim$470 nm at low [Hg^{2+}] and has a bathochromic shift to $\sim$500 nm at high [Hg^{2+}] (Fig. 4B); this behaviour is in agreement with the absence of a well defined isosbestic point in the absorption spectra and then with the formation of a complex whose structure changes with the salt concentration. Finally, the TCMA–Hg^{2+} complex in H_2O shows an emission centred at 506 nm, bathochromic shift of $\sim$20 nm if compared with the emission of TCMA itself.

The values of the fluorescence quantum yields of TCMA in the presence of the metal ions reported in Table 2 (ϕ_F = 0.0023–0.014) were measured at a salt concentration where the fluorescence intensity should have reached a plateau limit value (Fig. 4, insets). The quantum yield values show the very low efficiency of the emission process of the TCMA-ion complexes, even if it takes place from a singlet state localized on the methylacridinium moiety. This experiment allowed the

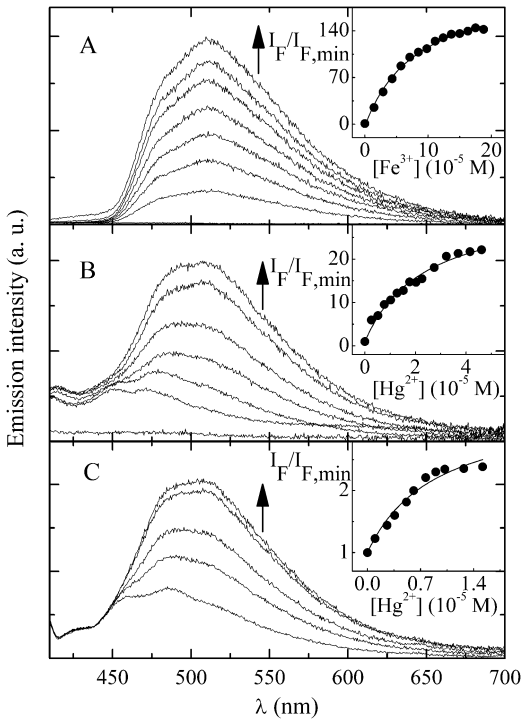

Fig. 4 Fluorescence emission of 6.0×10^{-6} M TCMA in MeCN in the presence of (A) $Fe(ClO_4)_3$ (0–8.8×10^{-4} M) and (B) $Hg(ClO_4)_2$ (0–4.6×10^{-5} M) and (C) in H_2O in the presence of $Hg(ClO_4)_2$ (0–1.5×10^{-5} M) (λ_{exc} = 358 nm); the full lines represent the best fittings obtained by use of eqn (1).

detection limit of $\sim 10^{-5}$ M and $\sim 10^{-6}$ M to be estimated for Fe^{3+} and Hg^{2+}, respectively.

The emission intensities were analyzed by use of eqn (1)[50] to determine the K_{ass} values (Fig. 4, insets):

$$I_F = \frac{I_{F,min} + I_{F,max} \times K_{ass} \times [ion]}{1 + K_{ass} \times [ion]} \quad (1)$$

where I_F is the fluorescence intensity upon anion addition, $I_{F,min}$ and $I_{F,max}$ are the fluorescence intensities of the free substrate and of the complex, respectively, and [ion] is the metal ion concentration in solution.

It has to be noted that the metal ion concentrations used in the above experiments were always significantly larger than those of TCMA and, therefore, the concentration of the complex in solution was much smaller than that of the free ion.

The measured association constants (Table 1) are in the 10 000–110 000 M^{-1} range. The K_{ass} values for the complexes with Hg^{2+} were larger than those obtained with Fe^{3+} and the values measured in H_2O were larger than those obtained in MeCN. This behaviour is in good agreement with the values of C_{50} recorded by spectrophotometric measurements for the same systems (Table 1), even if C_{50} obtained for the TCMA–Fe^{3+} in MeCN is slightly low in comparison with the corresponding K_{ass}.

It has to be noted that the ionic diameters of Fe^{3+} and Hg^{2+} are very different (1.24 Å and 2.2 Å, respectively). In fact, the small diameter of Fe^{3+} determines a high charge density and, subsequently, a strong electrostatic interaction with the lone pairs of the nitrogen and sulfur atoms of the crown moiety. Regarding Hg^{2+}, it is quite surprising to have such a strong association with TCMA, also taking into account that Ca^{2+}, an ion with a similar diameter (2.0 Å) and the same positive charge, does not interact at all with TCMA. This can be due to the different electronic structure of the cation and to the different ability to interact with planar ligands.

Despite paramagnetic ions such as Fe^{3+} being efficient fluorescent quenchers,[51,52] in this study the presence of Fe^{3+} induces emission; it has to be noted that this behavior is quite uncommon.[53] This is likely due to the particular effect of the cation on the nature of the emitting state. In fact, the forbidden emitting state of TCMA (CT nature) is replaced by the allowed π,π^* state in the TCMA/Fe^{3+} complex.

The interference effect due to the concomitant presence of different cations was not investigated in the present work. If the absence of absorption and emission spectral changes reflects the inability to form TCMA/cation complexes, the interference effect should be absent, as shown in the literature for other chemosensors.[54]

Even if an investigation of the pH effect was not carried out in great detail, the ability of TCMA to interact selectively with Hg^{2+} in aqueous solutions was still present at pH > 4 where the N atom of the crown was not protonated ($pK_a \approx 2.9$, calculated by the pK_a DB module of the program ACDLABS 11.0).

Femtosecond transient absorption

TCMA. The excited state dynamics of TCMA was investigated in MeCN by pump–probe absorption spectroscopy upon ultrafast excitation centred at 400 nm; the relatively low solubility of TCMA prevented the same measurements to be carried out in H_2O, too.

Taking into account the absorption spectrum of TCMA and the spectral broadening of the excitation pulses, hot vibrational levels of the lowest excited singlet states (mainly S_2) were populated upon excitation. The time-resolved absorption spectra of TCMA are shown in Fig. 5A while the decay kinetics recorded at two noteworthy wavelengths are shown in Fig. 6. The signals detected were negative, corresponding to bleaching of the ground state, between 500 and 625 nm in the region of the ground-state absorption and positive, corresponding to transient absorption, in the regions below 500 nm and above 625 nm. In fact, the recorded spectra show an hypsochromic shift in the position of the negative band in time. The growth kinetic recorded for TCMA at 575 nm is the mirror image of the decay kinetics recorded at 480 and 660 nm. Very similar spectral and kinetic properties were detected in the presence of increasing amounts (up to 0.001 M) of the metal ions Na^+, Co^{2+}, and Pb^{2+} (Table 3).

The kinetic traces were analyzed for each system at various wavelengths (the best fittings were obtained by a bi-exponential function convoluted with the instrumental response profile with a Gaussian shape). The global analysis of the decay kinetics also revealed the presence of two components (a short and a longer-lived one; S and L, respectively). The values of τ_S and τ_L are in the 0.50–0.96 ps and 3.3–3.9 ps ranges, respectively (Table 3). Furthermore, a

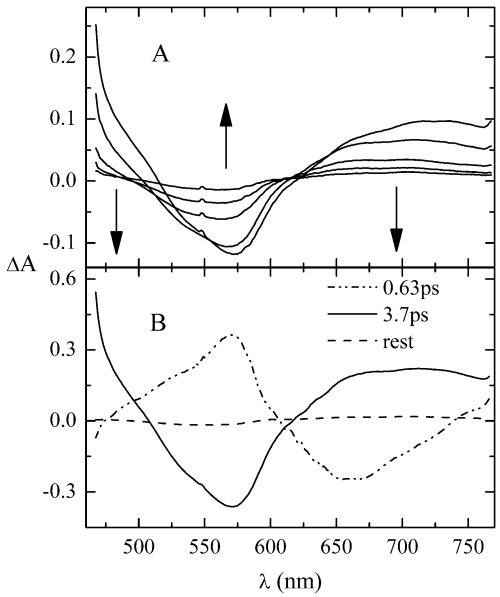

Fig. 5 (A) Pump–probe time-resolved absorption spectra of TCMA in MeCN recorded 1, 3, 5.5, 8.5 and 15 ps after the laser pulse (λ_{exc} = 400 nm). (B) Amplitudes of the decay components of TCMA in MeCN obtained by Global Analysis.

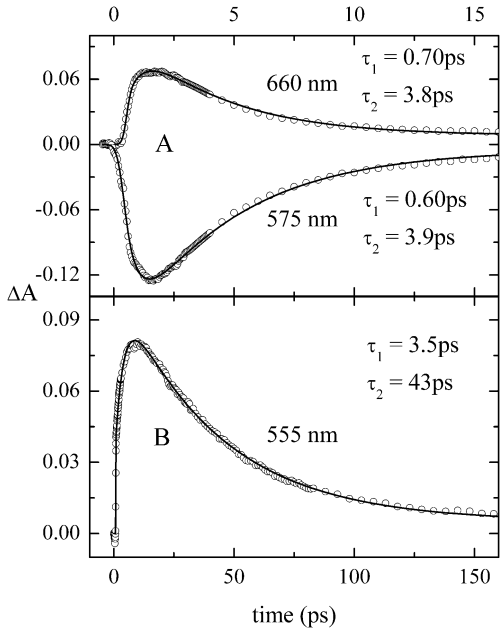

Fig. 6 Decay kinetics of (A) TCMA and (B) TCMA/Hg^{2+} (0.003 M) in MeCN (λ_{exc} = 400 nm). The full lines represent the best fittings obtained by bi-exponential functions.

very small and broad *rest* absorption replaced the longer lived component signal after its decay. These signals were not detected by ns laser flash photolysis measurements (see below).

The spectral shapes associated to S, L and to the *rest* absorption were calculated by using the SVD method followed by global analysis of the experimental data (see for example Fig. 5B). The S component exhibited negative amplitudes which are mirror images of the L component;

Table 3 Time constants of TCMA and TCMA/M^{n+} (0.001 M) systems in MeCN obtained by Global Fit (λ_{exc} = 400 nm)[a]

	S		L	
Metal	λ/nm	τ/ps	λ/nm	τ/ps
—	<460(−),570(+),660(−)	0.63	<460(+),570(−),700(+)	3.7
Na^+	<470(−),560(+),700(−)	0.50	<470(+),565(−),720(+)	3.8
Co^{2+}	<460(−),565(+),700(−)	0.96	<460(+),565(−),700(+)	3.3
Pb^{2+}	<470(−),570(+),710(−)	0.90	<470(+),570(−),710(+)	3.9
Hg^{2+}	<460(−),545(−),650(−)	3.7	<460(+),545(+),650(+)	45

[a] The symbols (+) and (−) stand for positive and negative signals, respectively.

these spectral properties are in agreement with a precursor–successor scheme which involves the S → L step.

Taking into account the data analysis and the time constants, the transient L was assigned to the lowest singlet state S_1 with charge transfer character (also characterized by the intense broad band centred at 552 nm in the ground-state absorption spectrum), while S, which is precursor of L, represents the quick solvent reorganization and $S_{2,v>0} \rightarrow S_{1,v=0}$ process after light absorption. The decay of L (S_1) is fast and it takes place by internal conversion (IC) followed by vibrational relaxation (VR). These findings confirm the absence of interactions between TCMA and Na^+, Co^{2+}, and Pb^{2+}; in fact, no spectral and kinetic changes were observed even at a high concentration of the metal ions.

TCMA/Hg^{2+}. In agreement with the steady-state measurements (see above), addition of Hg^{2+} changed significantly the spectral and kinetic properties of the lowest excited singlet states, thus indicating a different photophysical behaviour of the TCMA/Hg^{2+} complex. In fact, owing to the disappearance of the ground-state absorption band centred at 552 nm, only positive signals with maxima at <460 nm, 545 nm and 650 nm were recorded in these experimental conditions (see Fig. 7). Also in this case, the experimental data treated by SVD and Global Analysis revealed the presence of two components with spectral shapes shown in Fig. 7C (negative amplitudes for S and positive amplitudes for L) and lifetimes τ_S = 3.7 ps and τ_L = 45 ps (Table 3); Fig. 6B shows, as an example, a decay kinetics recorded at 555 nm together with the best fitting obtained with a bi-exponential function. Analogous to the other systems investigated, a very small *rest* absorption replaced the signal of the L component after its decay.

Considering the data analysis, the transient L was assigned to the lowest singlet state S_1 vibrationally relaxed, while S, which is precursor of L, represents the excited singlet state $S_{1,v>0}$ produced upon direct excitation at 400 nm which is quickly stabilized through solvent reorganization and vibrational cooling. Comparing the τ_L values recorded in these experiments, the decay of L ($S_{1,v=0}$), which takes place by fluorescence (*F*) and internal conversion (IC) followed by vibrational relaxation (VR), is slowed down by about one order of magnitude in the presence of Hg^{2+}.

The values of the radiative rate constant k_F calculated by the ratio ϕ_F/τ_F of TCMA and TCMA/Hg^{2+} are $\sim 1 \times 10^8$ and 0.5×10^8 s^{-1}, respectively, characteristic of allowed transitions.

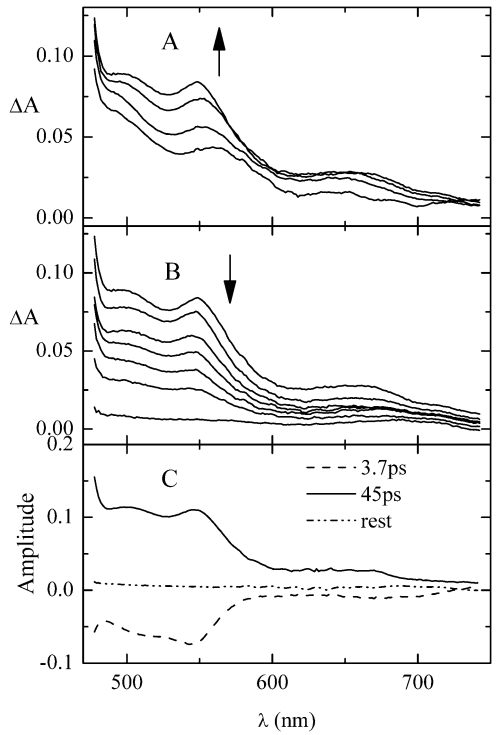

Fig. 7 Pump–probe time-resolved absorption spectra of TCMA/Hg^{2+} (0.001 M) in MeCN recorded (A) 1, 2, 4.5 and 10 ps and (B) 10, 20, 30, 40, 50, 70 and 250 ps after the laser pulse (λ_{exc} = 400 nm). (C) Amplitudes of the decay components of TCMA/Hg^{2+} (0.003 M) in MeCN obtained by Global Analysis.

The high photochemical reactivity of the TCMA–Fe^{3+} system upon irradiation with fs laser pulses prevented reliable kinetic and spectroscopic information to be obtained in MeCN.

Conclusions

The absorption spectrum of TCMA in a polar solvent is formed by a broad Vis band, due to the $S_0 \rightarrow S_1$ transition responsible for the violet colour of the solution and two structured bands due to the $S_0 \rightarrow S_2$ and $S_0 \rightarrow S_3$ transitions, characteristic of the methylacridinium moiety, at shorter wavelengths. The absorption in the Vis region is characterized by a charge-transfer nature with the methylacridinium moiety acting as the electron-acceptor and the anilic group as the electron-donor. No emission from the S_1 was detected both in MeCN and H_2O, while a small $S_2 \rightarrow S_0$ fluorescence emission (λ_{max} = 485 nm and ϕ_F = 0.0011) was detected in the aqueous medium. Time-resolved measurements with fs resolution of TCMA in MeCN have shown that the relaxed S_1 state is reached ~0.6 ps after the laser pulse, while the $S_1 \rightarrow S_0$ time constant (associated to the internal conversion process) is 3.7 ps.

The formation of complexes between metal ions and the crown thio-ether TCMA was shown both by spectrophotometric and spectrofluorimetric measurements. In particular, among the investigated metal ions, only Fe^{3+} and Hg^{2+} were able to form stable complexes with TCMA in a polar solvent. This was also shown by the switching of the solution colour from violet to yellow, owing to the disappearing of the 550 nm band and the increase of the absorption centred at 410 nm in the presence of Fe^{3+} or Hg^{2+}.

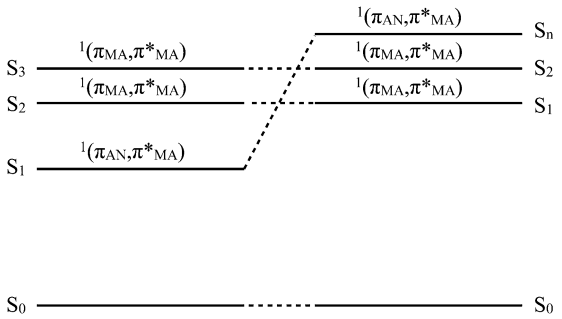

Scheme 2 State order of (left) TCMA and (right) TCMA/M^{n+} complexes.

The order and nature of the lowest excited singlet states of TCMA and their complexes with the metal ions are shown in Scheme 2.

As a matter of fact, it has already been reported that Ag^+ is able to interact more efficiently with crown thio- and aza-ethers rather than with crown ethers.[49] This behaviour cannot be understood by simply invoking electrostatic interactions because the negative charge on the etheroatoms of the crown decreases on going from oxygen to nitrogen and sulfur and then also the electrostatic interaction should decrease, as observed for alkali and alkaline earth metals. Taking also into account the ability of Ag^+ to form complexes with amines,[55] it is then probable that covalent bonds are involved in such complexes. Analogous behaviour could explain the strong interactions between Hg^{2+} and amines.[52] In fact, X-ray photoemission spectroscopy measurements have shown that the chemical interactions between Hg^{2+} and the sulfur atoms of crown thio-ethers in polymeric matrices involve the 4f electrons of the mercury ion and the 2p lone pairs of the S atoms.[56]

Contrarily to the behaviour in MeCN, addition of Fe^{3+} in H_2O did not modify the spectral properties of TCMA. The absence of interactions with TCMA can be ascribed to a competition between the hydration and the complexation processes of Fe^{3+} in the aqueous medium. Being this ion of *hard* type, it is strongly solvated by water (more polar than MeCN) and the interaction with TCMA becomes negligible.

The lowest excited singlet state of TCMA/M^{n+} complexes emits with low quantum yield (ϕ_F = 0.0023–0.014) and decays with time constants much longer than TCMA itself, at least in the case of TCMA/Hg^{2+} where it was possible to carry out time-resolved experiments with fs resolution.

Finally, this study showed the high selectivity of TCMA towards metal ions, the property which makes this compound a good candidate for colorimetric/fluorimetric sensing of Hg^{2+} (classified as *soft*) in aqueous media.

Acknowledgements

The authors gratefully acknowledge the financial support of the Ministero per l'Università e la Ricerca Scientifica e Tecnologica (Rome, Italy) and the University of Perugia [PRIN 2008, n. 20088NTBKR] and the Fondazione Cassa di Risparmio di Perugia.

Notes and references

1 B. Valeur and I. Leray, *Coord. Chem. Rev.*, 2000, **205**, 3–40.
2 A. P. de Silva, H. Q. N. Gunaratne, T. Gunnlaugsson, A. J. M. Huxley, C. P. McCoy, J. T. Rademacher and T. E. Rice, *Chem. Rev.*, 1997, **97**, 1515–1566.
3 J. F. Callan, A. P. de Silva and D. C. Magri, *Tetrahedron*, 2005, **61**, 8551–8588.
4 K. Tainaka, R. Sakaguchi, H. Hayashi, S. Nakano, F. F. Liew and T. Morii, *Sensors*, 2010, **10**, 1355–1376.
5 A. Minta, J. P. Y. Kao and R. Y. Tsien, *J. Biol. Chem.*, 1989, **264**, 8171–8178.
6 H. Komatsu, T. Miki, D. Citterio, T. Kubota, Y. Shindo, Y. Kitamura, K. Oka and K. Suzuki, *J. Am. Chem. Soc.*, 2005, **127**, 10798–10799.
7 X. Dong, Y. Yang, J. Sun, Z. Liu and B.-F. Liu, *Chem. Commun.*, 2009, 3883–3885.
8 M. Royzen, Z. Dai and J. W. Canary, *J. Am. Chem. Soc.*, 2005, **127**, 1612–1613.
9 M. Yu, M. Shi, Z. Chen, F. Li, X. Li, Y. Gao, J. Xu, H. Yang, Z. Zhou, T. Yi and C. Huang, *Chem.–Eur. J.*, 2008, **14**, 6892–6900.
10 M. Dong, T.-H. Ma, A.-J. Zhang, Y.-M. Dong, Y.-W. Wang and Y. Peng, *Dyes Pigm.*, 2010, **87**, 164–172.
11 H. S. Jung, P. S. Know, J. W. Lee, J. I. Kim, C. S. Hong, J. W. Kim, S. Yan, J. Y. Lee, J. H. Lee, T. Joo and J. S. Kim, *J. Am. Chem. Soc.*, 2009, **131**, 2008–2012.
12 E. M. Nolan and S. J. Lippard, *J. Am. Chem. Soc.*, 2003, **125**, 14270–14271.
13 S.-K. Ko, Y.-K. Yang, J. Tae and I. Shin, *J. Am. Chem. Soc.*, 2006, **128**, 14150–14155.
14 S. Yoon, E. W. Miller, Q. He, P. H. Do and C. J. Chang, *Angew. Chem., Int. Ed.*, 2007, **46**, 6658–6661.
15 X. Zhang, Y. Shiraishi and T. Hirai, *Tetrahedron Lett.*, 2008, **49**, 4178–4181.
16 P. D. Selid, H. Xu, E. M. Collins, M. S. Face-Collins and J. X. Zhao, *Sensors*, 2009, **9**, 5446–5459.
17 J. Fan, K. Guo, X. Peng, J. Du, J. Wang, S. Sun and H. Li, *Sens. Actuators, B*, 2009, **142**, 191–196.
18 E. M. Nolan, M. E. Racine and S. J. Lippard, *Inorg. Chem.*, 2006, **45**, 2742–2749.
19 S. Yoon, A. E. Alberts, A. P. Wong and C. J. Chang, *J. Am. Chem. Soc.*, 2005, **127**, 16030–16031.
20 M. Tian and H. Ihmels, *Chem. Commun.*, 2009, 3175–3177.
21 K. Kiyose, H. Kojima, Y. Urano and T. Nagano, *J. Am. Chem. Soc.*, 2006, **128**, 6548–6549.
22 C. J. Chang, J. Jaworski, E. M. Nolan, M. Sheng and S. J. Lippard, *Proc. Natl. Acad. Sci. U. S. A.*, 2004, **101**, 1129–1134.
23 E. Murphy, J. H. Bassett and G. R. Williams, *Practitioner*, 2006, **250**, 4–6.
24 P. G. Georgopoulos, A. Roy, M. J. Yonone–Lioy, R. E. Opiekun and P. J. Lioy, *J. Toxicol. Environ. Health, Part B*, 2001, **4**, 341–394.
25 R. von Burg, *J. Appl. Toxicol.*, 1995, **15**, 483–493.
26 T. W. Clarkson, L. Magos and G. J. Myers, *N. Engl. J. Med.*, 2003, **349**, 1731–1737.
27 J.-Y. Koh, *Mol. Neurobiol.*, 2001, **24**, 99–106.
28 P. D. Perrin, W. L. F. Amarego and D. R. Perrin, *Purification of Laboratory Chemicals*, Pergamon Press, Elmsford, 1980.
29 S. Guang, S. Yin, H. Xu, W. Zhu, Y. Gao and Y. Song, *Dyes Pigm.*, 2007, **73**, 285–291.
30 S. Yoon, A. E. Albers, A. P. Wong and C. J. Chang, *J. Am. Chem. Soc.*, 2005, **127**, 16030–16031.
31 R. E. Wolf, J. R. Artman, J. M. E. Storey, B. M. Foxman and S. R. Cooper, *J. Am. Chem. Soc.*, 1987, **109**, 4328–4335.
32 R. M. G. Roberts, D. Ostovic and M. M. Kreevoy, *Faraday Discuss. Chem. Soc.*, 1982, **74**, 257–265.
33 S. A. Jonker, F. Ariese and J. W. Verhoeven, *Recl. Trav. Chim. Pays-Bas*, 1989, **108**, 109–115.
34 M. Montalti, A. Credi, L. Prodi and M. T. Gandolfi, *Handbook of Photochemistry*, 3rd edn, (and references therein), CRC Press, Boca Raton, FL, 2006.
35 A. Barbafina, M. Amelia, L. Latterini, G. G. Aloisi and F. Elisei, *J. Phys. Chem. A*, 2009, **113**, 14514–14520.
36 T. DelGiacco, B. Carlotti, S. DeSolis, A. Barbafina and F. Elisei, *Phys. Chem. Chem. Phys.*, 2010, **12**, 8062–8070.
37 A. Barbafina, L. Latterini, B. Carlotti and F. Elisei, *J. Phys. Chem. A*, 2010, **114**(19), 5980–5984.
38 G. H. Golub and C. F. V. Loan, *Matrix Computations*, 2nd edn, Johns Hopkins University Press, Baltimore, 1989.
39 G. Strang, *Introduction to linear algebra*, Wellesley-Cambridge Press, Wellesley, MA, USA, 1998.
40 H. Gorner, F. Elisei and G. G. Aloisi, *J. Chem. Soc., Faraday Trans.*, 1992, **88**, 29–34.
41 A. Romani, F. Elisei, F. Masetti and G. Favaro, *J. Chem. Soc., Faraday Trans.*, 1992, **88**, 2147–2154.
42 M. C. Zerner, *Semiempirical molecular orbital methods*,in *Reviews in Computational Chemistry*, ed. K. B. Lipkowitz and D. B. Boyd, VCH, New York, 1991, Vol. 2, pp. 313–365.
43 J. J. P. Stewart, *J. Comput. Chem.*, 1989, **10**, 209–220.
44 J. J. P. Stewart, *J. Comput. Chem.*, 1989, **10**, 221–264.
45 S. Fukuzumi and T. Tanaka, in *Photoinduced Electron Transfer*, ed. M. A. Fox and M. Chanon, Elsevier, Amsterdam, 1988, Part C, p. 578.
46 T. L. Macdonald, W. G. Guteim, R. B. Martin and F. P. Guengerich, *Biochemistry*, 1989, **28**, 2071–2077.
47 T. G. Beaumont and K. M. C. Davis, *Nature*, 1970, **225**, 632.
48 S. A. Jonker, F. Ariese and J. W. Verhoeven, *Recl. Trav. Chim. Pays-Bas*, 1989, **108**, 109–115.
49 H. K. Frensdorff, *J. Am. Chem. Soc.*, 1971, **93**, 600–606.
50 R. D. Braun, *Introduction to Chemical Analysis*, McGraw-Hill, 1982.
51 J. H. Chang, Y. M. Choi and Y. K. Shin, *Bull. Korean Chem. Soc.*, 2001, **22**, 527–530.
52 J. H. Chang, Y. Jeong and Y. K. Shin, *Bull. Korean Chem. Soc.*, 2003, **24**, 119–122.
53 J. L. Bricks, A. Kovalchuk, C. Trieflinger, M. Nofz, M. Buschel, A. I. Tolmachev, J. Daub and K. Rurack, *J. Am. Chem. Soc.*, 2005, **127**, 13522–13529.
54 Y. Xiang and A. Tong, *Org. Lett.*, 2006, **8**, 1549–1552.
55 T. H. Wirth and N. Davidson, *J. Am. Chem. Soc.*, 1964, **86**, 4314–4318.
56 A. J. Nelson, J. G. Reynolds, T. F. Baumann and G. A. Fox, *Appl. Surf. Sci.*, 2000, **167**, 205–215.